ELSEVIER

Surface Science 430 (1999) 29–36

surface science

www.elsevier.nl/locate/susc

An infrared spectroscopic investigation of thin alumina films: measurement of acid sites and surface reactivity

M. Kaltchev, W.T. Tysoe *

Department of Chemistry and Laboratory for Surface Studies, University of Wisconsin-Milwaukee, Milwaukee, WI 53211, USA

Received 8 December 1998; accepted for publication 19 February 1999

Abstract

The surface chemical activity of an alumina films grown on Mo(100) by oxidation of aluminum evaporated onto the surface and oxidized using water is examined using Auger, X-ray photoelectron and reflection/absorption infrared spectroscopies. The formation of alumina is confirmed using Auger and X-ray photoelectron spectroscopy from the positions and intensities of the aluminum features and using reflection-absorption infrared spectroscopy from the longitudinal optical modes of the Al–O bonds measured at $\sim 935\ \mathrm{cm}^{-1}$. The presence of surface hydroxyls is monitored by forming films using D_2O which are evidenced by a feature at $\sim 2700\ \mathrm{cm}^{-1}$. Ammonia adsorption on a dehydroxylated surface yields a single peak at $1260\ \mathrm{cm}^{-1}$ due to ammonia adsorbed at a surface Lewis site where the principle symmetry axis of ammonia is oriented perpendicularly to the surface plane. Ammonia also appears to adsorb at Lewis sites on a hydroxylated surface with a slightly different adsorption geometry from that on a dehydroxylated surface. Finally, the chemistry of trimethyl aluminum adsorbed on the planar hydroxylated alumina surface is compared with that found on high-surface-area γ-alumina where the spectra and the chemistry found in both régimes is exactly identical except that the low-frequency methyl bending modes (at 769 and $718\ \mathrm{cm}^{-1}$) are not obscured on the thin film by the intense substrate whereas they are on the high-surface-area support.

Keywords: Acid sites; Alumina; Ammonia adsorption; Reflection-absorption infrared spectroscopy; Thin films; Trimethyl aluminum adsorption

1. Introduction

The growth and formation of oxide films for use, for example, as model catalyst supports have been extensively studied using a range of surface-sensitive techniques such as low-energy electron diffraction (LEED) [1], Auger and X-ray photoelectron spectroscopy (XPS) [2–4,6], scanning-tunneling microscopy (STM) [7] and high-resolution electron energy loss spectroscopy (HREELS) [3–5]. Adsorption onto these surfaces has also been studied [8,9]. Reflection-absorption infrared spectroscopy (RAIRS) has also been used to characterize thin alumina films [6,10,11]. These experiments have demonstrated that oxide films can be grown that reasonably mimic high-surface-area, supported systems. Infrared spectroscopy has also been extensively used to scrutinize the properties of high-surface-area oxides, for example, to examine changes in the extent of hydroxylation, titration of Lewis acid sites by Lewis bases such as ammonia, and to follow reactions at the surfaces of these oxides [12,13]. More recently, it has

---

* Corresponding author. Fax: +414-229-5036.
E-mail address: wtt@csd.uwm.edu (W.T. Tysoe)

PII: S0039-6028(99)00376-3

become possible to measure the infrared spectra of species adsorbed on the surface of planar single crystals using RAIRS which can furnish an infrared spectrum of a monolayer or less of a surface adsorbate. In the following, this technique is used to monitor the chemistry of thin alumina films grown on a molybdenum substrate formed by oxidizing aluminum by water in ultrahigh vacuum. It is possible to detect the longitudinal optical (LO) vibrations associated with the stretching of the Al–O bonds of a thin film of the oxide. It is also possible to use infrared spectroscopy to scrutinize the nature and type of the surface acid sites from the spectrum of basic adsorbates on planar alumina surfaces in exactly the same way as carried out previously using high-surface-area, γ-alumina and to follow surface reactions, specifically the thermal decomposition of trimethyl aluminum, on alumina.

2. Experimental

Alumina films are deposited onto a Mo(100) single crystal substrate by sequences of cycles of aluminum evaporation/water oxidation (with H_2O or D_2O). These cycles are necessary to ensure complete oxidation of aluminum which may be difficult to achieve with thicker aluminum layers. Oxidation is monitored using Auger electron spectroscopy (AES) and XPS. Aluminum is evaporated from a small heated alumina tube which is enclosed in a stainless-steel shroud to minimize contamination of other parts of the system [14]. Aluminum is evaporated onto the Mo(100) surface at 300 K for 120 s which, from measurements of the resulting oxide film thickness (see below), deposits ~1.5 monolayers. This is oxidized by water vapor (either H_2O or D_2O) at 650 K for 300 s. Water is supplied via a capillary doser to minimize background contamination. Calibration of the doser by comparing the coverage of CO on clean Mo(100) obtained by backfilling the chamber or from the dosing source reveals an effective pressure enhancement of ~200. This results in an effective water oxidation pressure of $\sim 2\times10^{-6}$ Torr. This procedure is repeated until a film of the desired thickness is formed. These experiments were carried out in a vacuum system that has been described in detail elsewhere [15]. Briefly, the main 12″-diameter, stainless-steel vacuum chamber was pumped by an ion and turbo-molecular pump and operates at a base pressure of $\sim 1\times10^{-10}$ Torr following bakeout. The chamber was equipped with a single-pass, cylindrical-mirror analyzer for Auger analysis of the sample and a quadrupole mass analyzer for temperature-programmed desorption experiments, leak testing and for gauging the purity of gases introduced into the chamber. Auger spectra were collected using an electron beam energy of 3 keV and a peak-to-peak modulation amplitude of 1 V. XPS data were collected using the double-pass cylindrical mirror analyzer operating at a pass energy of 50 eV. Mg Kα radiation was furnished by a water-cooled source operating at a power of 120 W. The chamber also contained a retractable, electron-beam heating filament which is used to heat the molybdenum substrate to ~2000 K for cleaning. The sample was mounted to the end of a horizontal sample manipulator which could be retracted to move the sample into a small-volume infrared cell. The sample could also be resistively heated, and cooled to ~80 K by pumping liquid nitrogen down the center of the sample transfer rod. The infrared apparatus was mounted on an optical table for stability and infrared radiation from a Midac Fourier-transform spectrometer was steered and focused onto the sample. The reflected light was collected and focused onto a cooled mercury–cadmium–telluride (MCT) detector and the resulting signal collected and analyzed by a microcomputer running SpectraCalc software. The optical path was completely covered by a dry-air-purged enclosure. The infrared radiation was furnished by an air-cooled source and spectra were collected with a resolution of $4\ \mathrm{cm}^{-1}$ for 1000 scans which typically took 4 min to accumulate.

The oxide film was generally grown in the main chamber and characterized using Auger and X-ray photoelectron spectroscopies. In order to avoid potential problems due to electron beam damage of the oxide films, once an effective film growth protocol had been established, fresh films were grown for infrared analysis. Infrared spectra were collected after retracting the sample from the preparation chamber into the infrared cell. This cell was also equipped with a directional dosing source consisting of a 2 mm-diameter capillary which could be used to deposit reactants onto the sample with minimal contamination of the background. The deionized water (H_2O) and deuterated water (D_2O, Aldrich, 95%) and oxygen (Matheson, 99.9%) used to oxidize the films were transferred to glass bottles. Normal water (H_2O) was generally used for surface oxidation. D_2O was used in experiments to observe surface hydroxyl modes to shift the frequency to a region of the spectrum where it could be observed using the MCT detector. The water was purified using repeated freeze–pump–thaw cycles and the oxygen was further purified by bulb-to-bulb distillations. Ammonia (Aldrich, 99.99%) was used directly from the cylinder without further purification. The trimethyl aluminum (Aldrich, 99%) was transferred from the cylinder to a glass bottle using a syringe inside a purged glove box and also then further cleaned using repeated freeze–pump–thaw cycles. The purity of all these compounds was tested using mass spectroscopy.

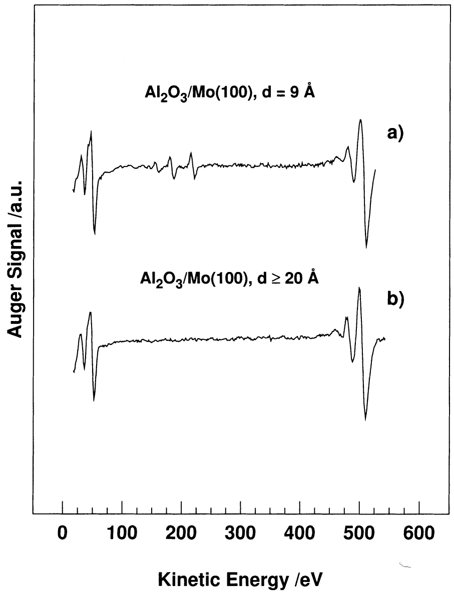

Fig. 1. Auger spectra of alumina deposited onto a Mo(100) substrate, in the presence of water (H_2O), for various times. The resulting estimated oxide film thickness is marked adjacent to each spectrum (see text).

3. Results

Fig. 1 displays a series of Auger spectra collected following different cycles of formation of alumina films by reaction between water (H_2O) and aluminum evaporated onto a clean Mo(100) substrate. Initially, the molybdenum substrate is still detected through the thin alumina films (Fig. 1a) where the molybdenum substrate is indicated by lines at 186 and 221 eV kinetic energy (KE) with a weaker line at 160 eV KE. The sharp peak at ~52 eV KE is assigned to the presence of aluminum and the peak at 510 eV is due to oxygen. A simple calculation of the relative intensities of the alumina and molybdenum features using the intensities of pure molybdenum and aluminum oxide collected using the same spectrometer, as well as the electron escape depths for the respective kinetics energies, allows the film thickness to be estimated [2]. The spectrum in Fig. 1a corresponds to a film of ~9.5 Å thick and the spectrum in Fig. 1b to a film >20 Å thick since the substrate is completely obscured. The binding energy of the aluminum Auger feature at ~52 eV is sensitive to aluminum oxidation state [16]. Both the absolute value of the peak position of aluminum metal (68 eV) as well as the associated fine structure are completely different from that of the film formed by reaction with water, confirming the presence of aluminum oxide (Fig. 1a and 1b). The ratio between the intensity of the oxygen Auger feature (510 eV KE) and that of aluminum (52 eV KE) is ~1.5 which is also in good agreement with the value measured by other workers [2]. The full oxidation of the film was confirmed using XPS. This exhibits an aluminum 2p feature at ~74 eV binding energy confirming the presence of an oxide [17,18].

The corresponding infrared spectrum of an alumina film formed using H_2O is displayed in Fig. 2a. This shows an intense feature centered at ~935 cm^{-1} which is somewhat asymmetric with a high-frequency tail that extends above 1000 cm^{-1}. This corresponds to LO vibrations of the Al–O bonds [6]. Note that, due to the surface selection rules, the transverse optical (TO)

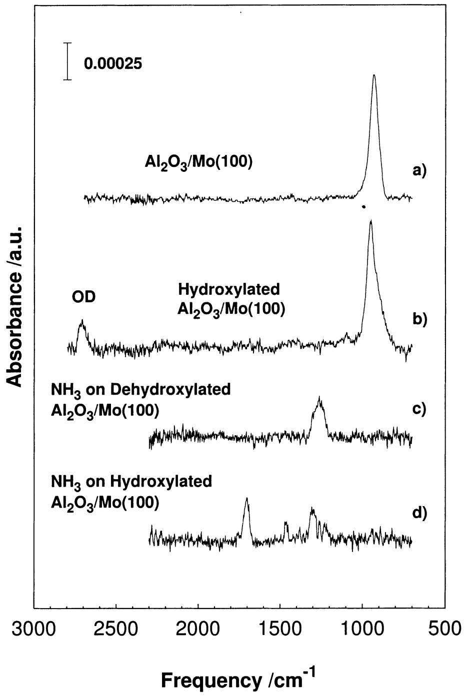

Fig. 2. RAIRS of (a) alumina grown on Mo(100) by reaction between aluminum and water (H_2O), (b) alumina grown on Mo(100) by reaction between aluminum and deuterium oxide (D_2O), (c) alumina grown on Mo(100) by reaction between aluminum and water (H_2O), annealed at 900 K to remove surface hydroxyls and exposed to ammonia at 80 K and annealed to 260 K and allowed to cool to 80 K when the spectrum was collected and (d) alumina grown on Mo(100) by reaction between aluminum and water and exposed to ammonia at 80 K and annealed to 220 K and allowed to cool to 80 K when the spectrum was collected. The absorbance scale in indicated by a vertical line in the figure.

vibrations are not observed. Fig. 2b shows the spectrum of a similar film after heating in vacuo to 850 K, then hydroxylating with deuterium oxide (D_2O) and heating again to 700 K to desorb any molecular water. The oxide vibrations are centered also at 960 cm^{-1} and the shape of the curve is slightly different, now having a tail to lower frequencies. This is an indication of a more-ordered, more γ-like Al_2O_3[6]. In addition, there is a clear feature centered at 2700 cm^{-1} which is assigned to an O–D stretching mode due to hydroxyl species present on the surface of the oxide film [19]. Shown in Fig. 1c is the spectrum obtained by exposing a dehydroxylated alumina film (obtained by heating to 900 K in vacuo to remove the surface hydroxyls), where the oxide was grown using H_2O, to ammonia. This exhibits a clear feature at 1260 cm^{-1} and is assigned to the deformation mode of ammonia adsorbed at Lewis sites of the alumina. Finally shown in Fig. 2d is the spectrum of ammonia adsorbed on hydroxylated alumina grown by reaction with water (H_2O) at 80 K and subsequently annealed to 225 K. This displays features at ~1710 cm^{-1} and a small peak at 1450 cm^{-1}. The feature at 1260 cm^{-1} now no longer consists of a single, broad feature but has more structure. Note that all of these spectra were collected at a sample temperature of 80 K.

Displayed in Fig. 3 are a series of spectra collected after exposing a hydroxylated alumina surface grown using water (H_2O) to ammonia at 80 K and then heating for a period of 5 s to various

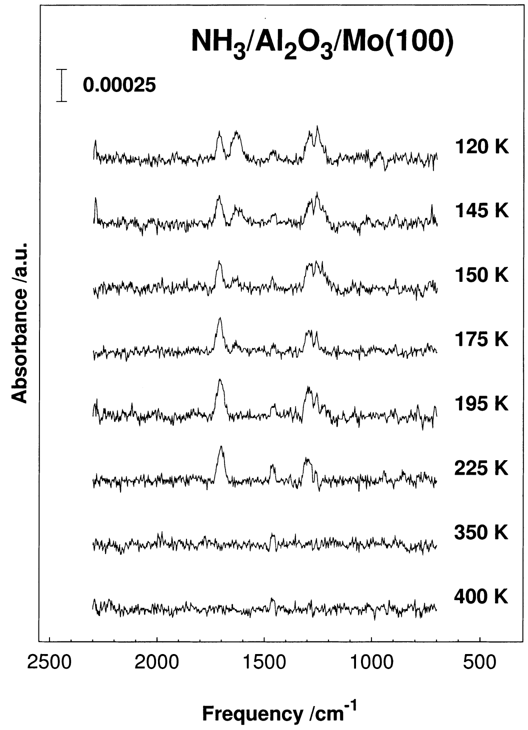

Fig. 3. Infrared spectrum of an alumina surface grown by reaction of aluminum and water (H_2O) on Mo(100) exposed to ammonia at 80 K and annealed to various temperatures for 5 s and allowed to cool to 80 K following which the spectrum was collected. The annealing temperature is shown adjacent to each spectrum.

temperatures after which the sample was allowed to cool to 80 K and the spectrum collected. At 120 K, the spectra exhibit peaks at 1714 and 1629 cm^{-1} as well as the broad feature at ~1260 cm^{-1} consisting of two features at 1257 and 1282 cm^{-1} and a narrow peak at ~1458 cm^{-1}. As the sample is warmed, the 1257 cm^{-1} feature disappears very rapidly and is completely absent after warming to 175 K. The 1629 cm^{-1} feature similarly decrease in intensity with increasing temperature so that the spectrum consists of a feature centered at 1710 cm^{-1} after heating to 225 K. The 1452 cm^{-1} feature grows on warming sample to 225 K and, above this temperature, all of the other feature disappear while the 1452 cm^{-1} peak remains up to 400 K.

Finally, shown in Fig. 4 are a series of spectra of an alumina surface grown by reaction between aluminum and water (H_2O) on Mo(100) which was then exposed to trimethyl aluminum at 80 K. This exhibits a number of reasonably intense modes at 718, 769, 1198 and 1248 cm^{-1}. All of these modes can be assigned to dimeric trimethyl aluminum and the frequencies and their assignments are summarized in Table 1 [20]. The sample was then heated to the temperature marked adjacent to each of the spectra for a period of 5 s and allowed to cool to 80 K following which the spectrum was recorded. As the sample is warmed to 190 K, all of the features decrease in intensity indicating that some of the trimethyl aluminum desorbs from the surface. In addition, the 1248 cm^{-1} mode decreases in intensity substantially more rapidly than does that at 1189 cm^{-1} so that on heating to 240 K, this region of the spectrum consists entirely of a broad feature at 1206 cm^{-1}. Similarly, the 769 cm^{-1} peak decreases rapidly in intensity so that only a 719 cm^{-1} feature persists at 240 K. As the sample is heated further to room temperature (300 K), the spectrum consists of a features at 1218 and 719 cm^{-1}. Shown also are spectra collected following adsorption of trimethyl aluminum on hydroxylated, high-surface-area, γ-alumina which exhibits a peak at 1209 cm^{-1} following adsorption at 300 K, which is in very good agreement with the spectra of planar samples collected in ultrahigh vacuum. Note that adsorbate modes below ~1100 cm^{-1}

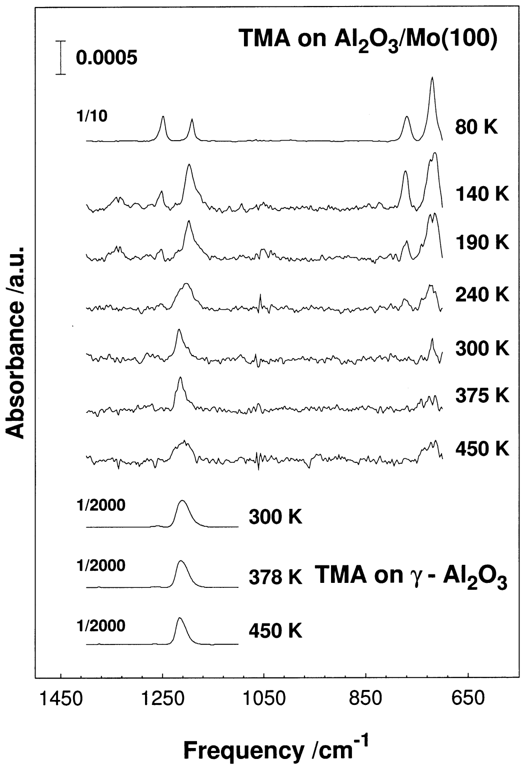

Fig. 4. RAIRS of a hydroxylated alumina surface grown by reaction between alumina and water (H_2O) on a Mo(100) surface exposed to trimethyl aluminum at 80 K. The subsequent spectra were collected by heating the sample to various temperatures in vacuo for 5 s and allowing the sample to cool to 80 K, following which the infrared spectrum was collected. The annealing temperature is marked adjacent to each spectrum. Shown also are spectra of trimethyl aluminum on high-surface-area γ-alumina exposed at 300 K and annealed in vacuo to higher temperatures. Again, sample temperatures are shown adjacent to each spectrum.

Table 1
Assignments of frequencies of the infrared spectrum formed by the adsorption of trimethyl aluminum on alumina grown on Mo(100)

Frequency (cm^{-1})	Assignment
718	$\rho(CH_3)$, A_u, B_u
769	$\rho(CH_3)$, A_u
1198	$\delta_s(CH_3)$, A_u, B_u
1254	$\delta_s(CH_3)$, B_u

are obscured by the alumina lattice modes on the high-surface-area sample whereas they are easily detectable on the thin film.

4. Discussion

The Auger spectroscopic data of Fig. 1 confirm that thin oxide films can be grown on Mo(100) by evaporating aluminum in the presence of water where layers from a few Angstroms to >20 Å can be grown in a controlled manner. These data are confirmed by XPS. Strong lattice modes can be observed at $\sim 935\ \mathrm{cm}^{-1}$ (Fig. 2a) and this spectrum is in good agreement with that found using RAIRS of oxidized aluminum and this feature is therefore assigned to the Al–O LO modes [6]. Note that these modes are also observed on high-surface-area alumina and are sufficiently intense that it is essentially impossible to detect adsorbate vibrations on high-surface-area alumina below $\sim 1100\ \mathrm{cm}^{-1}$.

The alumina surface can be hydroxylated and OH groups are formed at the surface by growing the alumina from water. Such sites are identified in infrared spectroscopy from their characteristic OH stretching features at $\sim 3750\ \mathrm{cm}^{-1}$ [10,11]. This is out of the range that can be accessed with the MCT detector used for these experiments. However, substituting deuterium for hydrogen should shift this peak to $\sim 2700\ \mathrm{cm}^{-1}$ and the resulting spectrum for surface hydroxyls formed by hydroxylating an alumina layer with deuterated water is displayed in Fig. 2b and clearly shows the O–D stretching mode at $2700\ \mathrm{cm}^{-1}$ [19]. The corresponding frequency of the bending mode of gas-phase D_2O is at $1178\ \mathrm{cm}^{-1}$ [21] and is not seen in Fig. 2b indicating the complete absence of any molecular water on the surface. Note that this is assigned to the presence of hydroxylated alumina since the $960\ \mathrm{cm}^{-1}$ lattice modes are characteristic of bulk Al–O modes for alumina.

Surface acidic sites can be measured by titrating them with a base and ammonia is commonly used for this purpose. In this case, both Brønsted and Lewis sites can be detected where NH_4^+ is formed in the former case and adsorbed NH_3 in the latter. Infrared spectroscopy has been used to detect the presence of ammonia from the N–H bending modes and the exact frequencies of this mode gives an indication of the strength of the Lewis acid site [22]. The ν_2 (a_1) mode of ammonia (at $\sim 950\ \mathrm{cm}^{-1}$ in the gas phase [23]) is very sensitive to the acid strength of the oxide to which it is coordinated: the greater the electron–acceptor power, the greater the shift of ν_2 to higher frequencies. Fig. 2c displays the spectrum found by exposing an alumina surface, grown by oxidizing an aluminum film with H_2O, to ammonia and this yields a clear feature at $1260\ \mathrm{cm}^{-1}$ which is characteristic of ammonia adsorption on Lewis sites on alumina. Accompanying this mode, and generally much more intense, is another mode at $\sim 1628\ \mathrm{cm}^{-1}$ which is not evident in Fig. 2c. In our case, however, ammonia adsorbs on a planar alumina substrate grown on a metal layer so that the surface selection rules apply, where only vibrational modes perpendicular to the surface are detected. The ν_2 mode has a_1 (z) symmetry whereas the $1628\ \mathrm{cm}^{-1}$ peak (ν_4) has e (x, y) symmetry in the C_{3v} point group. This suggests that this mode is symmetry forbidden with this experimental arrangement and that the C_3 axis of the adsorbed ammonia is perpendicular to the sample plane. This situation is different to that on the hydroxylated surface (Figs. 2d and 3) where many more modes are detected. In this case, the 1257 and $1629\ \mathrm{cm}^{-1}$ modes decrease identically with increasing temperature, as do the 1282 and $1714\ \mathrm{cm}^{-1}$ modes. The $1629\ \mathrm{cm}^{-1}$ peak can be assigned to the ν_2 mode of ammonia adsorbed at Lewis sites also identified on dehydroxylated alumina (Fig. 2c). In this case, the corresponding ν_4 mode is evident at $1629\ \mathrm{cm}^{-1}$ whereas it is completely absent on dehydroxylated alumina (Fig. 2c). This suggests that the C_3 rotation axis of adsorbed ammonia is no longer perpendicular to the plane of the sample and that the ammonia orientation is affected by hydroxylation of the surface. The frequency of the ν_4 mode at $1629\ \mathrm{cm}^{-1}$ is generally not strongly perturbed by adsorption onto the surface and has a larger absorption cross section than the ν_2 ($1257\ \mathrm{cm}^{-1}$) mode [22]. This suggests that the tilt angle of the principle axis of ammonia on Lewis sites on hydroxylated alumina is relatively small. This ammonia is also much more weakly adsorbed than on the dehydroxylated surface since it is completely removed by heating to 195 K.

The assignment of the 1282 and 1714 cm^{-1} features is less clear. The 1282 cm^{-1} peak could be due to a shifted ν_2 mode of ammonia adsorbed at a Lewis site. However, the corresponding ν_4 mode would be expected at ~1628 cm^{-1} whereas the associated peak is at 1714 cm^{-1}. As noted above, the frequency of the ν_4 mode changes only very slightly on adsorption so this peak is unlikely to be due to this vibrational mode. Interestingly, the mode at ~1450 cm^{-1} (Fig. 3) observed following ammonia adsorption has been taken to be characteristic of NH_4^+ [22]. However, alumina is not generally considered to have strong Brønsted sites which would be required for the formation of NH_4^+ species that persist at annealing temperature up to 400 K.

Chemical reactions can also be monitored in a similar way on the thin-film oxide surface as illustrated by the data in Fig. 4 which displays the infrared spectrum of trimethyl aluminum adsorbed on the alumina film grown using H_2O compared with the corresponding spectrum obtained on high-surface-area alumina [24]. Of particular note is the fact that the thin oxide layer allows the low-frequency methyl rocking modes at 718 and 769 cm^{-1} to be detected whereas these are obscured on the high-surface-area samples by the intense substrate absorption. The 1248 and 1198 cm^{-1} features are due to methyl bending modes, the 1248 cm^{-1} peak being due to the bridging methyl species in the trimethyl aluminum dimer and the 1198 cm^{-1} mode due to the terminal species. As the sample is heated, all of the features decrease in intensity so that the 1248 cm^{-1} feature is completely absent on warming the sample to 300 K indicating dissociation of the trimethyl aluminum dimer into monomers. The 1198 cm^{-1} mode also shifts to 1218 cm^{-1} indicative of thermal decomposition. This shift has been shown to correspond to the decomposition of an adsorbed dimethyl aluminum species into monomethyl aluminum [24]. These results indicate that the chemistry of trimethyl aluminum is identical on the thin film grown in ultrahigh vacuum to that found on high-surface-area alumina when this sample is exposed to trimethyl aluminum vapor. It has recently been shown that similar results are obtained when alumina powder is immersed in a solution of metal alkyl (in this case dimethyl zinc [25]) so this strategy allows the sample chemistry to be followed over a wide range of conditions from ultrahigh vacuum, through intermediate pressures on high-surface-area pellets to solutions.

5. Conclusions

Thin films of alumina deposited onto a Mo(100) in ultrahigh vacuum can be characterized using RAIRS by examining the lattice phonons and also by observing hydroxyl species directly from their infrared modes and by observing Lewis sites from the infrared spectrum of ammonia absorbed on the surface. In addition, the chemistry of trimethyl aluminum on these thin-film oxide surfaces is very similar to that found on high-surface-area alumina.

Acknowledgements

The authors gratefully acknowledge partial support of this work by the US Department of Energy, Division of Chemical Sciences, Office of Basic Energy Sciences, under Grant No. DE-FG02-92ER14289. They also thank Professor J.J. Fripiat for useful discussions.

References

[1] P.J. Chen, D.W. Goodman, Surf. Sci. 312 (1994) L767.
[2] H.H. Madden, D.W. Goodman, Surf. Sci. 150 (1985) 39.
[3] P.J. Chen, M.L. Colaianni, J.T. Yates Jr., Phys. Rev. B 41 (1990) 8025.
[4] B.G. Frederick, G. Apai, T.N. Rhodin, Surf. Sci. 244 (1991) 67.
[5] T.N. Rhodin, B.G. Frederick, G. Apai, Surf. Sci. 287 (1993) 638.
[6] C. Brüesch, R. Kötz, N. Neff, L. Pietronero, Phys. Rev. B 29 (1984) 4691.
[7] C. Xu, W.S. Oh, G. Liu, D.Y. Kim, D.W. Goodman, J. Vac. Sci. Technol. A 15 (3) (1997) 1261.
[8] T.N. Rhodin, R.P. Merril, P.J. O'Hagan, S.C. Woronick,

N.D. Shinn, G.L. Woolery, A.W. Chester, J. Phys. Chem. 98 (1994) 2433.
[9] B.G. Frederick, G. Apai, T.N. Rhodin, Surf. Sci. 277 (1992) 337.
[10] A.J. Maeland, R. Rittenhause, W. Lahar, P.V. Romano, Thin Solid Films 21 (1974) 67.
[11] F.P. Mertens, Surf. Sci. 71 (1978) 161.
[12] J.B. Peri, J. Phys. Chem. 69 (1965) 211.
[13] J.B. Peri, J. Phys. Chem. 69 (1965) 231.
[14] W.J. Wytenburg, R.M. Lambert, J. Vac. Sci. Technol. A 10 (1992) 3597.
[15] M.G. Kaltchev, A. Thompson, W.T. Tysoe, Surf. Sci. 391 (1997) 145.
[16] C.D. Wagner, Handbook of Auger Electron Spectroscopy, Perkin-Elmer, Eden Prairie, MN, 1987.
[17] T. Barr, Appl. Surf. Sci. 15 (1983) 1.
[18] C.D. Wagner, D.E. Passoja, H.F. Hillery, T.G. Kinsky, H.A. Six, W.T. Jansen, J.A. Taylor, J. Vac. Sci. Technol. 21 (1982) 933.
[19] A.V. Kiselev, V.I. Lygin, in: D. Slutzkin (Ed.), Infrared Spectra of Surface Compounds, Wiley, New York, 1975.
[20] T. Ogawa, Spectrochimica 24A (1968) 15.
[21] T. Shimanouchi, Tables of Molecular Vibrational Frequencies vol. 1, National Bureau of Standards, Gaithersburg, MD, 1972, pp. 1–60.
[22] F. Yin, A.L. Blumenfeld, V. Gruver, J.J. Fripiat, J. Phys. Chem. 101 (1997) 1824.
[23] G. Herzberg, Infrared and Raman Spectra of Polyatomic Molecules, van Nostrand, New York, 1951.
[24] C. Soto, R. Wu, D.W. Bennett, W.T. Tysoe, Chem. Mater. 6 (1994) 1705.
[25] V. Boiadjiev, W.T. Tysoe, in preparation.